An ionic liquid imprinted nanocomposite adsorbent: Simulation, kinetics and thermodynamic studies of triclosan endocrine disturbing water contaminant removal

***Imran Ali [1,2], Gunel T . Imanova[3], Hassan M Albishri[2], Wael Hamad Alshitari[4] and Marcello Locatelli[5]**

[1]Department of Chemistry, Jamia Millia Islamia (Central University), Jamia Nagar, New Delhi, 110025, India

[2]Department of Chemistry, King Abdulaziz University, Jeddah, Saudi Arabia

[3]Department of Physical, Mathematical and Technical Sciences, Institute of Radiation Problems, Azerbaijan National Academy of Sciences, AZ 1143, Baku, Azerbaijan

[4]Department of Chemistry, College of Science, University of Jeddah, P.O. 80327, Jeddah, 21589, Saudi Arabia

[5]Analytical and Bioanalytical Chemistry, University "G. d'Annunzio" of Chieti-Pescara; Department of Pharmacy, Build B, level 2; Via dei Vestini, 31; 66100 Chieti, Italy

Abstract:

The presence of triclosan in water is toxic to human beings, hazards to the environment and creates side effects and problems because this is an endocrine disturbing water pollutant. Therefore, there is a great need for the separation of this notorious water pollutant at an effective, economic and eco-friendly level. The interface sorption was achieved on synthesized ionic liquid-based nanocomposites. *N*-methyl butyl imidazolium bromide ionic liquid copper oxide nanocomposite was prepared by green methods and characterized by using proper spectroscopic methods. The nanocomposite was used to remove triclosan in water with the best conditions of time 30 minutes, concentration 100 µg/L, pH 8.0, dose 1.0 g/L, and temperature 25 °C; with 90.2% removal capacity. The results obeyed Langmuir, Temkin and D-Rs isotherms with first-order kinetic and liquid film diffusion kinetic model. The positive entropy value was 0.47 kJ/mol K while the negative value of enthalpy was -0.11 kJ/mol. The negative values of free energy were -53.18, -74.17 and -76.14 kJ/mol at 20, 25 and 30 °C. These values confirmed exothermic and spontaneous sorption of triclosan. The combined effects of 3 D parameters were also discussed. The supramolecular model was developed by simulation and chemical studies and suggested electrovalent bonding between triclosan and N-methyl butyl imidazolium bromide ionic liquid. Finally, this method is assumed as valuable for the elimination of triclosan in water.

Keywords: Ionic liquid Nanocomposite, Water treatment, Endocrine disturbing triclosan, Simulation, Thermodynamics and kinetics.

***: Correspondence:** drimran.chral@gmail.com; drimran_ali@yahoo.com

1. Introduction:

Nowadays, new generation water pollutants are getting more attention for their removal. And these are personal care products, medicinal, and pharmaceuticals residues. Among many residues, triclosan has been found as a water pollutant in some places of the world [1]. Also, this compound has been reported in some aquatic animals [2,3]. Basically, triclosan is used as an antimicrobial agent with a wide range of activities. It is used as oral medicine in some countries [4]. It is mixed with many personal products during their preparation. Most commonly triclosan is mixed with sanitizers, soaps, skin cream, etc. [5]. It is also used in houses, hotels and hospitals to maintain hygiene [6-11]. Besides, it is also used as an additive in polymer making such as polyethylene and polyolefin polymers. Consequently, there are great chances of water contamination by triclosan. It is a pollutant of high concern because of its endocrine disturbing nature. A good value of log K_{ow} of 4.8 octanol-water partition coefficient made it capable to be bioaccumulative in fatty tissues, which is responsible for toxicity. Besides, the hormonal activity of these pollutants is studied *in vitro* and *in vivo* (animals) and showed serious effects [12-15]. These effects may be on human beings. The most notorious effect is that triclosan may enter into the human body through body skin [16,17], which may be a dangerous sign for health. Briefly, triclosan is a serious and toxic pollutant and its detailed health hazards are discussed by Olaniyan et al. [1]. Chemically triclosan is known as 5-Chloro-2-(2,4-dichlorophenoxy)phenol (Figure 1) with $C_{12}H_7Cl_3O_2$ molecular formula and 289.54 g/mol as molecular weight.

Due to the above discussion, it is very clear that there is an urgent need for fast, economic, reproducible and reliable methods for the removal of triclosan n water. Among many methods of water treatment, adsorption is gaining importance day by day as evident from a large number of publications every year [18-22]. Some papers are available on the removal of triclosan. Brose et al. [23] defined triclosan removal in influent, effluent, and biosolids. Wu et al. [24] defined the subtraction of triclosan using clay and sandy soils with maximum sorption at a high concentration of 0.05 mg/L. Besides, the maximum sorption was at low pH, which is not the pH of natural water.

Moreover, the authors reported maximum sorption in days, which is a high time for fast and economic processes. Tonga et al. [25] described the removal of triclosan using biosolids derived biochar. The authors reported high sorption at low pH. Khori et al. [26] reported the removal of triclosan by using activated carbon prepared from waste biomass. Although the equilibrium achieved was within 20 minutes but the adsorption capacity was low *i.e.* 80.77%. Fard and Barkdoll [27] reported the removal of triclosan on magnetic nanoparticles. The authors reported maximum removal in 47 minutes. Yi et al. [28] reported the removal of triclosan using core-shell Fe_3O_4@COFs nanoparticles. The removal was good but the adsorbent is costly and it is difficult to use on a large scale. Triwiswaraa et al. [29] reported the removal of triclosan by using char obtained from palm kernel. The authors reported maximum sorption from 6 to 12 hrs, which is a high time period for a fast and economic process. Jiang et al. [30] reported the removal of triclosan on the silica-zeolite sorbent. The authors reported the removal of triclosan at a high concentration of about 2.0 mico mole. It is clear from the above-cited literature that no one can be used to remove this pollutant on a large scale economically. The reason is that almost all methods took a longer time, which is not feasible in natural water treatment on a large scale. Moreover, mostly, methods are applicable at high concentrations of triclosan while it is present at the microgram level in the water. Keeping these facts into consideration, a new *N*-methyl butyl imidazolium bromide ionic liquid-based copper oxide nanocomposite was prepared by the facile and green method. The nanocomposite was characterized and used for the removal of triclosan. The sorption mechanism was developed by simulation and chemical methods. The results of the findings are discussed in this article.

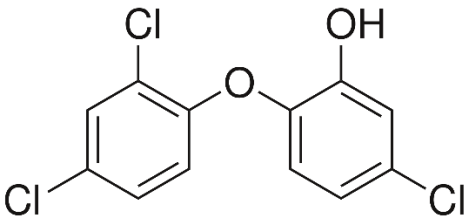

Figure 1: Structure of triclosan.

2. Experimental:

The detail of the chemicals, reagents, instruments used and experimental protocol is given in Supplementary Information. However, some important information is provided herein.

2.1 Preparation of N-methyl butyl imidazolium bromide CuO nanocomposite

Copper nanoparticles were prepared by green methods by utilizing the appropriate amount of copper acetate and *Acacia arabica* leave extract. 50 g leaves of *Acacia arabica* were dried in shade, ground in the form of water paste and heated in 1000 mL distilled water at 80 °C for 2 hrs followed by cooling at room temperature and filtration through Whatman filter paper number 1. 250 mL solution of copper acetate of 0.1 M concentration was prepared and the leave extract (500 mL) was mixed slowly with constant stirring. The pH of the solution was adjusted to 10 by using dilute sodium hydroxide solution. The solution was stirred for 5 hrs and kept stand undisturbed at room temperature. The solid part of the solution was centrifuged and washed with water following its activation in a furnace at 500 °C for 5 hrs. The so-formed nanoparticles of CuO were used to prepare the composite with N-methyl butyl imidazolium bromide. 0.5 g CuO nanoparticles were suspended in 100 mL water and after that, a solution of *N*-methyl butyl imidazolium bromide in 50 mL of the concentration of 1.0 g/L was added into a suspension of CuO nanoparticles. The solution was continued for string. The mixture was stirred for a further 2-3 hrs with constant heating. A blackish product was obtained which was washed with hot water and ethanol. Finally, the product was dried in an oven at 100 °C and used for further sorption studies.

2.2 Characterization of N-methyl butyl imidazolium bromide nanocomposite

The obtained *N*-methyl butyl imidazolium bromide ionic liquid copper oxide nanocomposite was characterized by FT-IR, XRD, SEM and TEM spectroscopic techniques. These methods were utilized as per the typical protocol.

2.3 Sorption study

The uptake capability of *N*-methyl butyl imidazolium bromide ionic liquid copper oxide nanocomposite was determined by the typical measures of batch mode. Several factors were

optimized and these were the amount of triclosan, sorbent dose, medium pH, time of contact and temperature. These variables used were 20-120 µg/L triclosan; 0.1-1.5 g/L for *N*-methyl butyl imidazolium bromide copper oxide nanocomposite dosage; 3-12 medium pHs; time of 5-40 minutes with a temperature of 20-30 °C. The lasting triclosan was detected by HPLC as described in the supplementary information. The different models are also given in supporting information to analysis the results. The equilibrium capacity of sorption was fixed by the following equation.

$$Q_e\ (\mu g/g) = (C_i - C_e).v/m \quad (1)$$

where C_i and C_e are starting and equilibrium amounts of triclosan in µg/L whilst m is the weight of *N*-methyl butyl imidazolium bromide copper oxide nanocomposite in g/L. The solution volume (v) was in a milliliter. Triclosan dismissal efficacy was measured by the given equation.

$$\text{Elimination}\ (\%) = [(C_i - C_t)/ C_0].100 \quad (2)$$

2.4 Kinetic study

The kinetic study of triclosan removal by *N*-methyl butyl imidazolium bromide copper oxide nanocomposite was fixed at 5 to 40 minutes by taking a known quantity of *N*-methyl butyl imidazolium bromide copper oxide nanocomposite with triclosan solution in a water bath which was temperature-controlled. The experiments were performed till the equilibrium was archived. The amount of triclosan was determined at dissimilar time periods. The trials were completed in a similar method as for the sorption ones.

2.5 Thermodynamics study

This sort of the study of triclosan was performed by using 20, 25 and 30 °C temperatures. The adjusted quantities of triclosan were utilized under these conditions.

2.6 Analysis of triclosan by HPLC

The residual quantities of the triclosan were estimated by HPLC procedure asgiven in the supplementary information (SI). The mobile phase used was 2.5 pH acetic acid buffer-acetonitrile (30:70) with 1.0 mL/min flow rate. The column used was Sunniest RP Aqua C_{28} (25 cm x 4.6 mm id) and detection was achieved at 280 nm. The identification of triclosan was determined by

equating the retention time of the standard with sample ones. The retention time of triclosan was 11.35 minutes.

2.7 Simulation study

The simulation docking of triclosan uptake was performed as per the typical method as given in supplementary information.

3. Results and discussion

3.1 Characterization

N-methyl butyl imidazolium bromide copper oxide nanocomposite was characterized by FT-IR. The peaks seen were at 455 and 500, which are due to the stretching vibration of Cu-O in CuO. No peak was seen in the 600 to 610 region; confirming the non-availability of Cu_2O [32]. A broadband at 3466 cm^{-1} was because of the sorbed water molecule. This information is an indication of the monoclinic structure of CuO. Besides these, peaks related to *N*-methyl butyl imidazolium bromide were also seen. The peaks at 690, 1760 and 3059 cm^{-1} were the characteristic of alkyl and imidazole ring C–H stretch. The results are in agreement with Wu et al. [33] findings. The crystallinity of the prepared *N*-methyl butyl imidazolium bromide copper oxide nanoparticles was ascertained by XRD studies and confirmed the presence of 110, 002, 200, 112, 202, 020, 202, 311 and 113 at 2θ values of 32, 36, 42, 47, 50, 55, 57, 65 and 68. These values are the confirmation of monoclinic hexagonal crystalline CuO. The crystal size was calculated by the following formula.

$D = K\lambda/dCos\theta$

where, d, θ, K and D are full width at half maximum, reflection angle, and constant; usually taken as 0.94. λ = 0.154 nm for Cu-Kα, β. The particles sizes calculated were from 50 to 98.5 nm.

The morphology of the prepared *N*-methyl butyl imidazolium bromide copper oxide nanoparticles was ascertained by SEM and the two photographs at 10,000 and 2,00,000 magnifications; showing the crystalline and rough surface. The shapes of the particles were irregular spherical. Another study for characterization was TEM and the picture is shown in Figure 2; confirming the round and irregular shape of nanoparticles with sizes ranging from 50 to 99.5 nm. These results are in promise with the XRD results. Based on the above argument, the following *N*-methyl butyl imidazolium bromide copper oxide nanoparticles structure (Figure 3) was developed in which four molecules of *N*-methyl butyl imidazolium bromide are found on the exterior of CuO. This structure has a positive charge and a very good sorbent for negatively charged species.

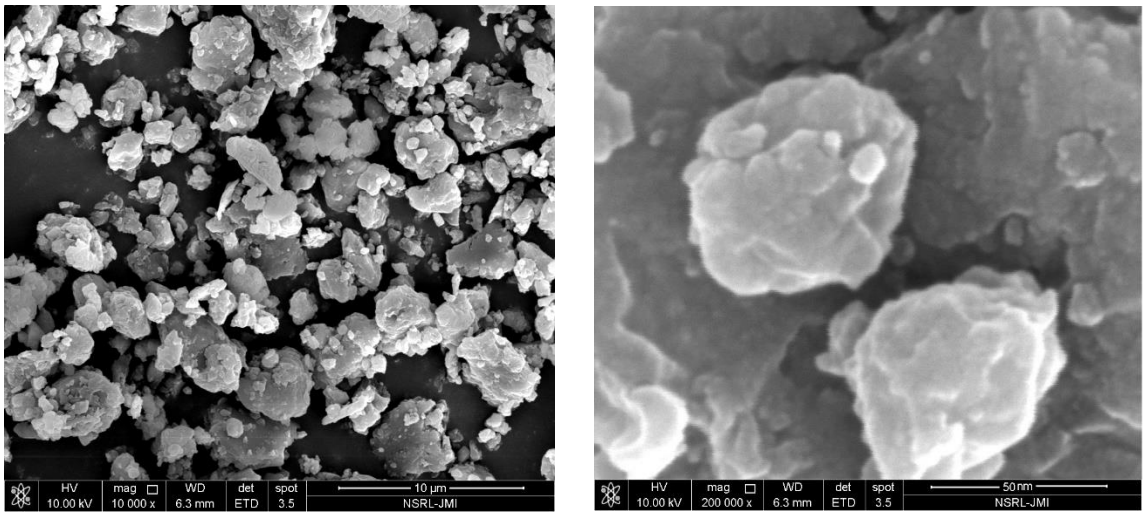

(a) **(b)**

Figure 2. SEM images of spectrum of *N*-methyl butyl imidazolium bromide copper oxide nanocomposite, (a): at 10,000 and (b): 2,00,000 magnifications.

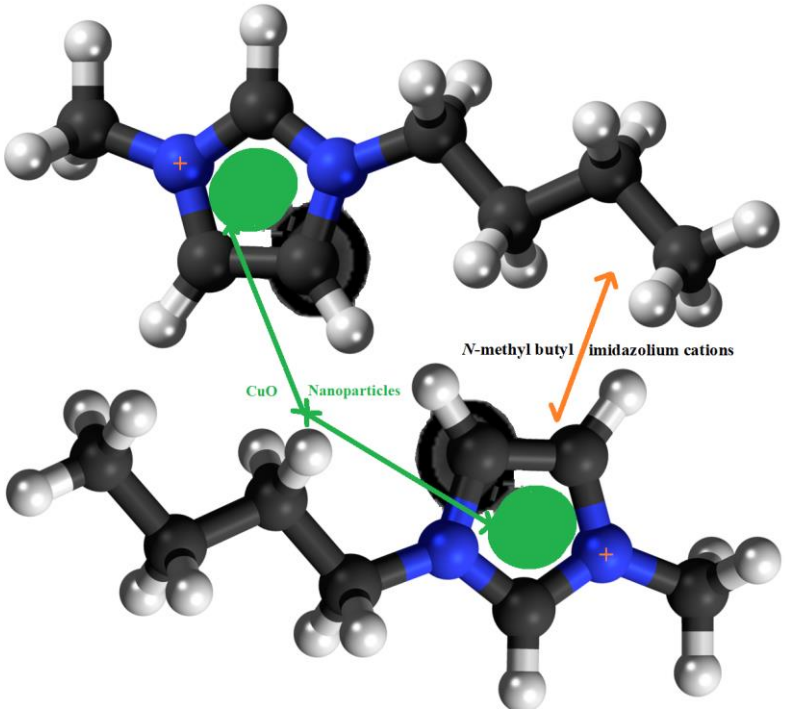

Figure 3. The structure of *N*-methyl butyl imidazolium cation copper oxide nanocomposite.

3.2 Sorption study

The uptake of triclosan was optimized by numerous parameters. The improved parameters were 20-120 µg/L triclosan; 0.1-1.5 g/L for *N*-methyl butyl imidazolium bromide copper oxide nanocomposite dosage; 3-12 medium pHs; time of 5-40 minutes with a temperature of 20-30 °C. The results of all these sets of experiments are given in the following sections.

3.2.1 Concentration of triclosan

The concentration of triclosan was optimized by taking 10 to 130 µg/L. The other variable controlled were contact time 30 minutes, pH 7.0, dose 1.0 and 25 °C temperature. The results of these sets of experiments findings are graphed in Figure 4a and it is clear from this Figure that the triclosan removal incased from 10 to 100 g/L concentration while further augment in the concentration could not result of more triclosan uptake. The sorption of triclosan were 9, 18.7, 28, 36, 45, 53.4, 63, 71.5, 80.5, 90.2, 90.3, 90.3 and 90.3 µg/g at 10, 20, 30, 40, 50, 60, 70, 80, 90, 100, 110, 120 and and 130 µg/L concentrations. The percentage calculations were done and the percentage removal at equilibrium was 90.2. This data is a confirmation of the fact that 100 µg/L

concentration was the optimized one at equilibrium. Therefore, 100 µg/L concentration of triclosan was considered as the best one in this set of experiments.

3.2.2 Contact time

The contact time for triclosan removal was optimized by taking 5 to 40 minutes. The other variable controlled were starting concentration 100 µg/L, pH 8.0, dose 1.0 and 25 °C temperature. The results of these sets of experiments findings are graphed in Figure 4b and it is clear from this Figure that the triclosan removal incased from 5 to 30 minutes time while further augment in the contact time could not result in more triclosan uptake. The sorption of triclosan were 13.6, 27.9, 42.5, 57.15, 72.90, 90.2, 91.3 and 91.3 µg/g at 5, 10, 15, 20, 25, 30, and 40 minutes. The percentage calculations were done and the percentage removals were 13.6, 27.9, 42.5, 57.15, 72.90, 90.2, 91.3 and 91.3. This data is confirmation of the fact that 30 minutes of contact time was the optimized one at equilibrium. Therefore, 30 minutes contact time for triclosan was considered the best one in this set of experiments.

3.2.3 pH of the solution

The solution pH for triclosan removal was optimized by taking 3 to 12 units. The other variable controlled were starting concentration 100 µg/L, contact time 30 minutes, dose 1.0 and 25 °C temperature. The results of these sets of experiments findings are graphed in Figure 4c and it is clear from this Figure that the triclosan removal incased from 3 to 8 pH while further augment in the pH could not result in more triclosan uptake. The sorptions of triclosan were 22.3, 32.4, 41.5, 57.4, 83.6, 91.2, 93.2, 93.3, 94.5 and 94.4 µg/g at 3, 4, 5, 6, 7, 8, 9, 10, 11 and 12 pH. The percentage calculations were done and the percentage removals were were 22.3, 32.4, 41.5, 57.4, 83.6, 91.2, 93.2, 93.3, 94.5 and 94.4. This data is a confirmation of the fact that 8.0 pH was the optimized one at equilibrium. Therefore, 8.0 pH for triclosan was considered the best one in this set of experiments. It is important to emphasize that many natural water resources have 7-8 pH and, therefore, it may be concluded that the given method may be highly useful to the natural water systems.

3.2.4 Dose of the nanocomposite

The nanocomposite dose for triclosan removal was optimized by taking 0.1, 0.25, 0.50, 0.75, 1.0, 1.25 and 1.5 g/L concentration. The other variable controlled were starting concentration 100 µg/L, contact time 30 minutes, pH 8.0 and 25 °C temperature. The results of these sets of experiments findings are graphed in Figure 4d and it is clear from this Figure that the triclosan removal incased from 0.1 to 1.0 g/L while further augment in dose could not result in more triclosan uptake. The sorptions of triclosan were 35.6, 55.4, 72.8, 81.7, 91.2, 91.2 and 92.4 µg/g at 0.1, 0.25, 0.50, 0.75, 1.0, 1.25 and 1.50 g/L. The percentage calculations were done and the percentage removals were 35.6, 55.4, 72.8, 81.7, 91.2, 91.2 and 92.4. This data is a confirmation of the fact that 1.0 g/L dose was the optimized one at equilibrium. Therefore, 1.0 g/L dose for triclosan was considered as the best one in this set of experiments.

3.2.5 Temperature of the solution

The experimental temperature for triclosan removal was optimized by taking 20, 25 and 30 °C. The other variable controlled were starting concentration 100 µg/L, contact time 30 minutes, 1.0 g/L dose and pH 7.0. The results of these sets of experiments findings are graphed in Figure 4e and it is clear from this Figure that the triclosan removal decreased from 20 to 30 °C while the experiments at further increased or decreased temperature were not done because these are not the temperatures of the natural water resources. The sorptions of triclosan were 9.0, 18.7, 28.5, 37.0, 46.4, 54.7, 64.2, 72.8, 82.2, 91.5, 92.3 and 92.3 µg/g at 20 °C while these values at 25 °C were 9.0, 18.7, 28.0, 36, 45, 53.4, 63, 71.5, 80.5, 90.2, 90.3, and 90.3 µg/g. The values at 30 °C were 9.0, 18.7, 26.8, 35, 43.6, 51.5, 60.4, 70.1, 79.5, 88.5, 88.3 and 88.2 µg/g. This data is confirmation of the fact that the sorption was in the order of 20 > 25 > 30 °C; confirming the exothermic sorption of triclosan on the reported nanocomposite.

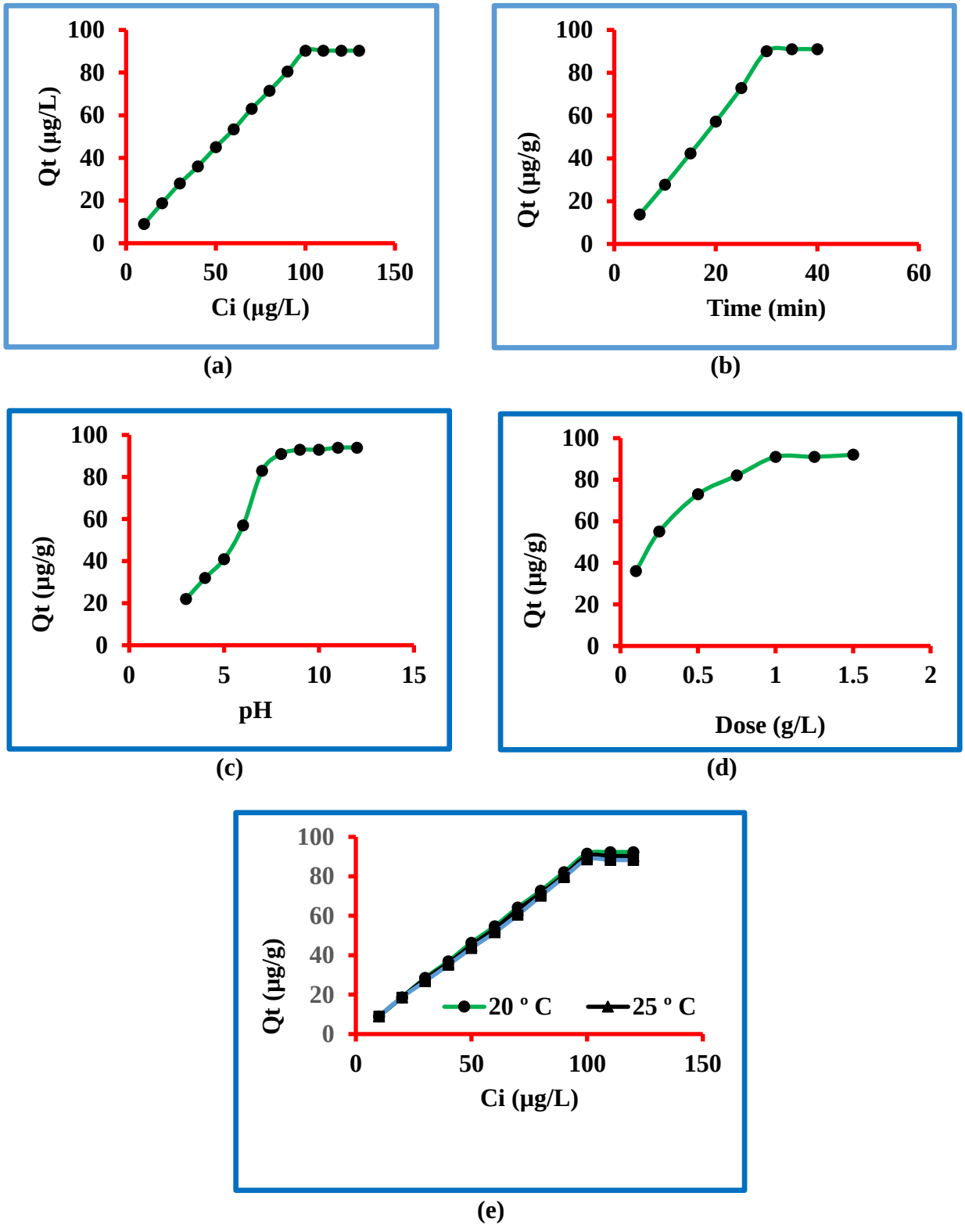

Figure 4: Sorption of triclosan (a) amounts, (b) ctime, (c) pH, (d) dose and (e) temperature.

3.3 Combined effect of the 3 D parameters

pH is one of the most important factors for determining the applicability of the method in the treatment of water in real-life problems. Therefore, efforts are made to study the combined effect of pH with initial concentration, time, dose, and temperature. The results are given in Fig. 5. A look at Figure 5a indicates that the best removal was 90.2% at 100 µg/L concentration and pH 8. Further increase in both concentration and pH could not augment the removal of triclosan. Similarly, a look at Figure 5b indicates that the best removal was 90.0% at 30 minutes and pH 8. Further increase in both contact time and pH could not augment the removal of triclosan. A look at Figure 5c indicates that the best removal was 91.0% at a 1.0 g/L dose and pH 8. Further increase in both dose and pH could not augment the removal of triclosan. Besides, the effects of %removal vs temperature vs pH are shown in Figure 5d, which indicates that the best removal was 91.5% at 20 ºC temperature and pH 8. Further increase in pH could not augment the sorption of triclosan. It is interesting to mention that the adsorption decreased at high temperatures. Therefore it was decided to select 25 ºC temperature throughout in this study because this is the temperature of most of the water resources. Finally, 25 ºC temperature was selected to carry out all the experiments and the maximum sorption of triclosan was 91.0% at pH 8.

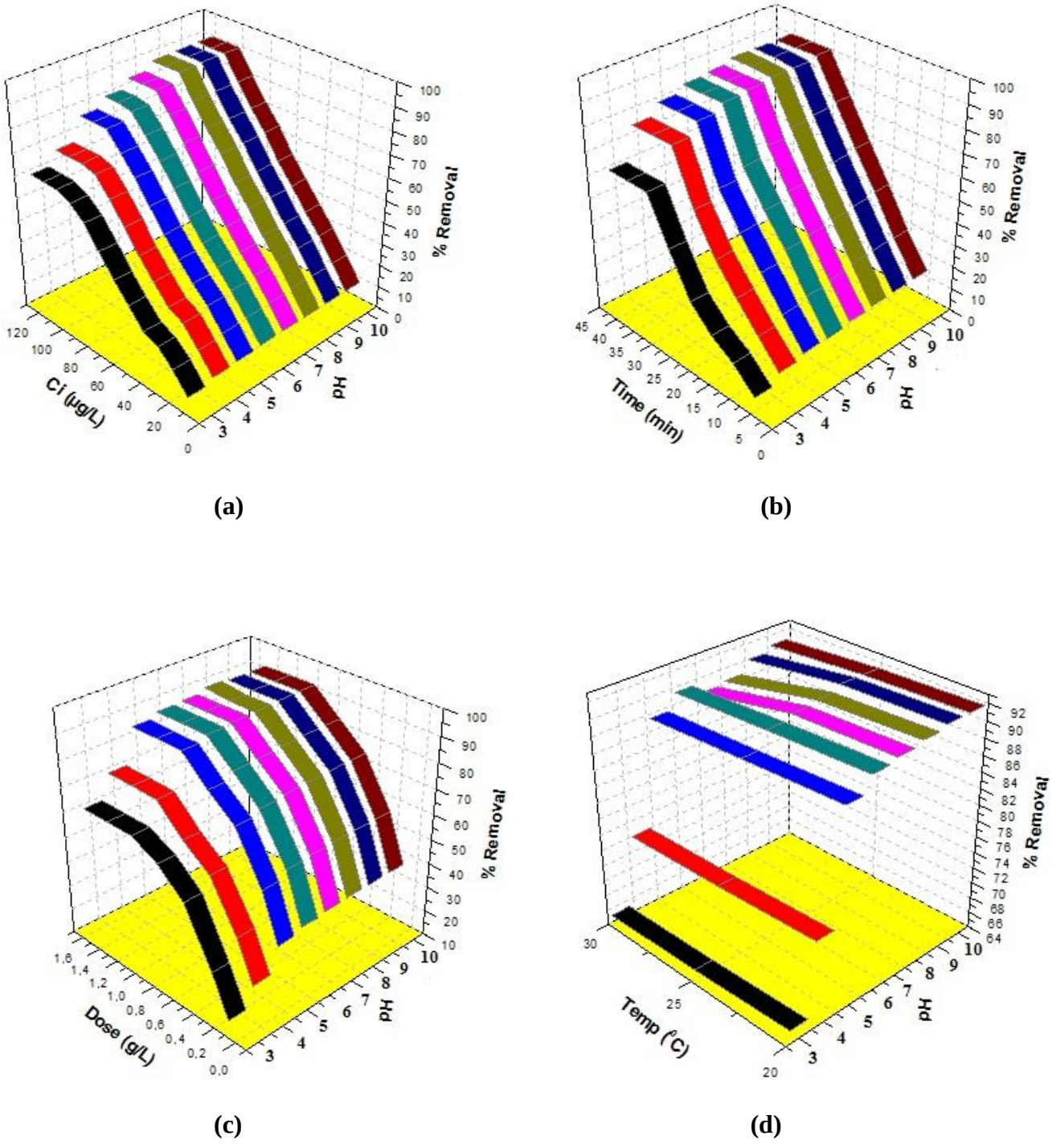

Figure 5. 3D plots for triclosan removal, (a): %removal vs Ci vs pH, (b): %removal vs time vs pH, (c) %removal vs dose vs pH and (d): %removal vs ttemperature vs pH.

3.4 Modeling

The data obtained after experiments were used to run the models and the most significant isotherms used were Langmuir, Freundlich, Temkin and Dubinin-Radushkevich. The findings after running these models are given below.

3.4.1 Langmuir

The equation of the Langmuir model is given in supplementary information (Table S1) and this equation was used to model the experimental data. The Langmuir model parameters were determined and expressed by b (L/µg) and X_m (µg/g). The magnitudes of these parameters were exploited by the intercept and slope of the plot drawn between $1/Q_t$ and $1/C_t$ (Figure 6a). These values are presented in Table 1, which confirmed 0.087, 0.015 and 0.008 µg/g values of X_{max} at 20, 25 and 30 °C, respectively, while the values of b were 188.68, 625 and 833.33 L/µg at these temperatures. The magnitude of regressing constants were 0.929, 0.967 and 0.901.

3.4.2 Freundlich

The equation of the Freundlich model is given in supplementary information (Table S1) and this equation was used to model the experimental data. The Freundlich model parameters were determined and expressed n (µg/L) and k_F (µg/g) (Figure 6b). The magnitudes of these parameters were exploited by intercept and slope of the plot drawn between logQt vs logCt. These values are presented in Table 1, which confirmed 17.64, 10.11 and 5.08 µg/g values of k_F at 20, 25 and 30 °C, respectively, while the values of n were 1.38, 1.09 and 0.89 L/µg at these temperatures. The magnitude of regressing constants were 0.949, 0.968 and 0.885. The out of the experimental data by Freundlich and Langmuir models were studied. A comparison can be seen in Table 1 and it is clear that the regression constants for Langmuir are close to unity in comparison to the Freundlich. It means that the experimental data followed the criterion of Langmuir model rather than Freundlich one. Finally, it was concluded that the sorption process proceeded by Langmuir model.

3.4.3 Temkin

The equation of Temkin model is given in supplementary information (Table S1) and this equation was used to model the experimental data. The Temkin model parameters were determined and expressed by K_T (L/µg) B_T and (kJ/mol) constants. The magnitudes of these parameters were exploited by slope and intercept of the plot drawn between logQt vs logCt (Figure 6c). These values are presented in Table 1, which confirmed 5.55, 2.99 and 1.86 L/µg of K_T at 20, 25 and 30

°C, respectively, while 3.35, 2.70 and 2.23 were the values of B_T at 20, 25 and 30 °C, respectively. The magnitude of regressing constants were 0.949, 0.968 and 0.885 at K_T at 20, 25 and 30 °C, respectively. These values are approaching the unity, which is the confirmation of the validity of the data by Temkinn model.

3.4.4 Dubinin-Radushkevich

The equation of Dubinin-Radushkevich model is given in supplementary information (Table S1) and this equation was used to model the experimental data. The Dubinin-Radushkevich model parameters were determined and expressed by Q_m (µg/g), K_{ad} (mol^2/kJ^2) and E (kJ/mol). The values of Q_m (µg/g) and E (kJ/mol) were determined by the intercept and slope of the plot drawn between the graph of $1/Q_t$ and $1/C_t$ (Figure 6d). The degrees of K_{ad} (mol^2/kJ^2) were computed by exploiting an equation as given below.

$$\ln Q_e = \ln Q_m - Kad.E^2 \qquad -3$$

where, Q_e, Q_m and E have the usual meaning.

The values of different constants are presented in Table 1, which confirmed 128.83, 158.48 and 177.83 µg/g of Q_m at 20, 25 and 30 °C, respectively, while 1.22, 3.20 and 5.83 mol^2/kJ^2 were the values of K_{ad} at 20, 25 and 30 °C, respectively. The degrees of E were 0.53, 0.42 and 0.36 kJ/mol at 20, 25 and 30 °C, respectively. The magnitude of regressing constants were 0.901, 0.954 and 0.849 at K_T at 20, 25 and 30 °C, respectively. These values are approaching to the unity, which is the confirmation of the validity of the data by the Dubinin-Radushkevich model.

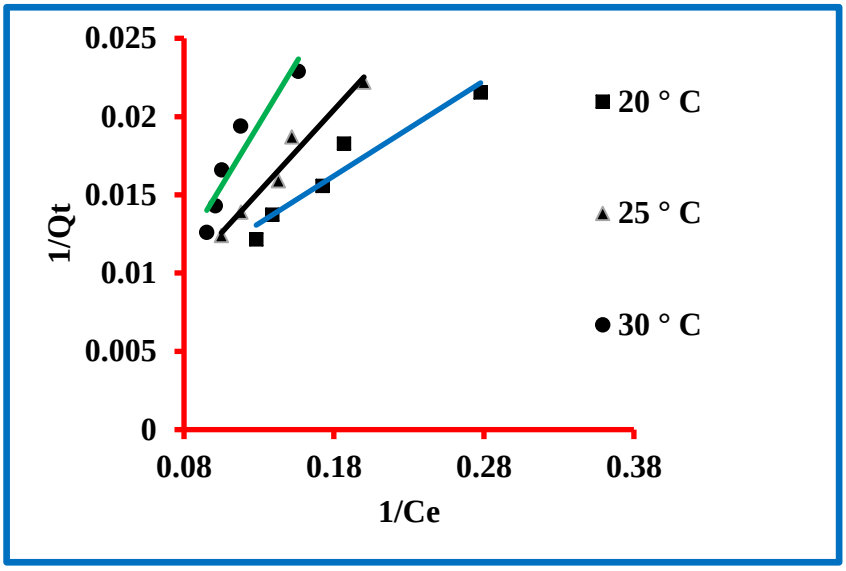
0.025
0.02
0.015
0.01
0.005
0
1/Qt
0.08
0.18
0.28
0.38
1/Ce
20 ° C
25 ° C
30 ° C

(a)

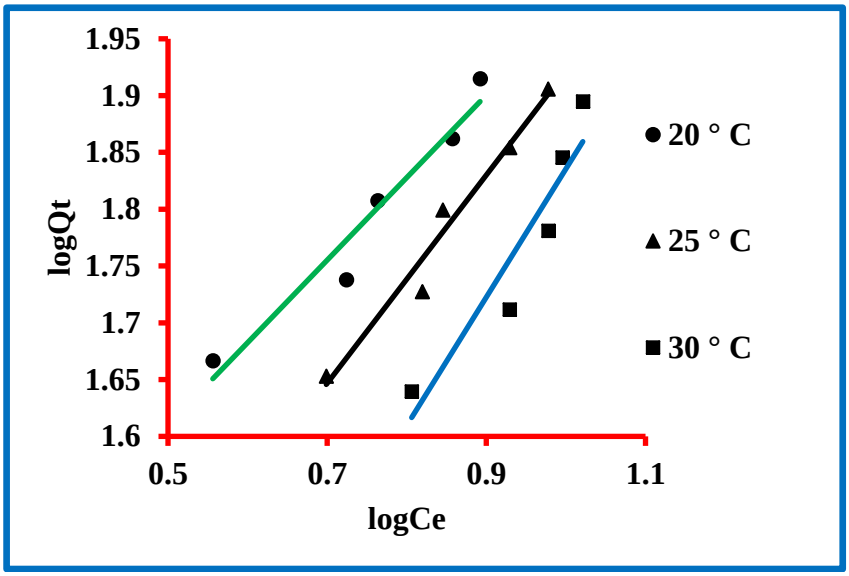
1.95
1.9
1.85
1.8
1.75
1.7
1.65
1.6
logQt
0.5
0.7
0.9
1.1
logCe
20 ° C
25 ° C
30 ° C

(b)

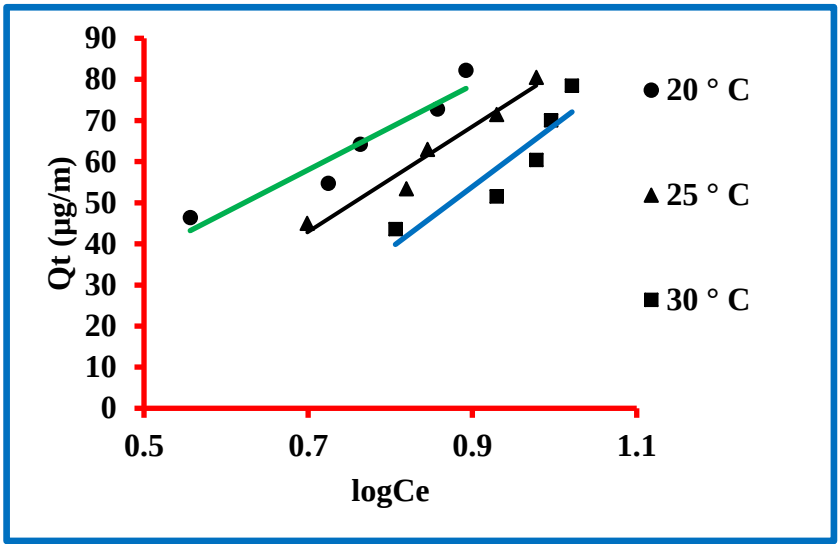

(c)

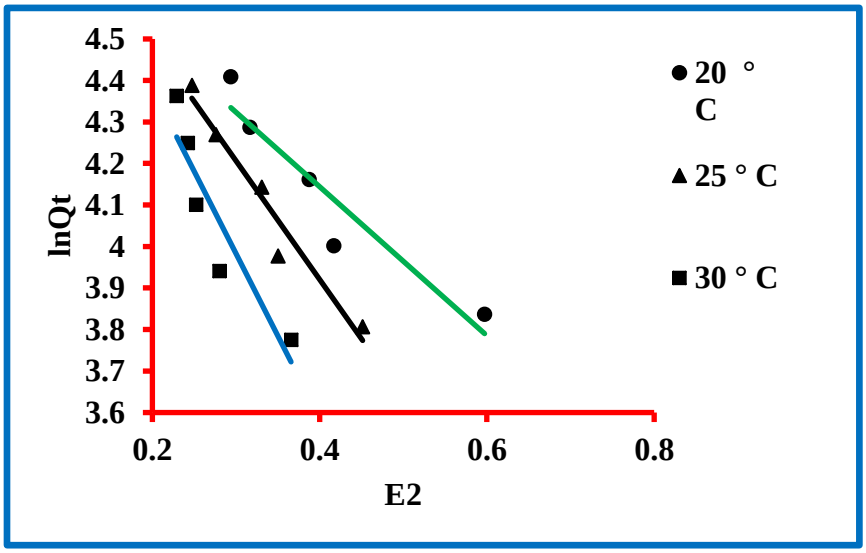

(d)

Figure 6: Models for triclosan, (a): Langmuir, (b) Freundlich, (c): Temkin and ((d): tetracycline and (d) Dubinin-Radushkevich.

Table 1: The adsorption isotherm parameters of triclosan.

Isotherms	Temperatures		
	20.0 ℃	**25.0 ℃**	**30.0 ℃**
Langmuir			
X_{max} (µg/g)	0.087	0.015	0.008
b (L/µg)	188.68	625	833.33
R^2	0.929	0.967	0.901
Freundlich			
k_F (µg/g)	17.64	10.11	5.08
n (µg/L)	1.38	1.09	0.89
R^2	0.949	0.968	0.885
Temkin			
K_T (L/µg)	5.55	2.99	1.86
B_T (kJ/mol)	3.35	2.70	2.23
R^2	0.949	0.968	0.885
D-R			
Q_m (µg/g)	128.83	158.48	177.83
K_{ad} (mol^2/kJ^2)	1.22	3.20	5.38
E (kJ/mol)	0.53	0.42	0.36
R^2	0.901	0.954	0.849

3.5 Kinetic Study

First, second and Elovich's kinetic models were exploited for computing the kinetics of the triclosan sorption process. The equations used for these models are given in SI (Table S2). First, second and Elovich's kinetic models graphs are plotted between log(Q_e-Q_t), t vs Qt and t, lnt vs Qt, respectively. The slopes and intercepts of these plots were exploited to compute the degrees of the various constants. The values of these different constants are presented in Table 2. Taking the example of first-order the values of rate constant was 0.073 1/min with 90.2 experimental and 124.11 theoretical values of the equilibrium concentration of triclosan. These values varied from each other by 33.91; confirming their closeness. The value of the regression constant was 0.995; approaching unity. Taking the example of second-order the values of rate constant was 3.26 x 10^{-6} g/µg min with 90.2 experimental value and 909.09 theoretical value. These values varied from each other by 818.89% confirming their non-closeness. The value of h was 2.70 µg/g min; confirming the good value of the initial rate of the sorption. The value of the regression constant was 0.994. The data of the first- and second-pseudo-order reaction models were matched. It was observed that the experimental and theoretical degrees of the sorbed triclosan amount were in

confidence in the first pseudo order reaction than the second-pseudo-order reaction model. Also, the degrees of the regression constants of triclosan were slightly higher in the case of first-order in comparison to the second-order reaction. Consequently, it was decided that the investigational data obeyed the first -pseudo-kinetic reaction. The degrees of adsorption (α) and desorption (β) rates were computed by Elovich's kinetic model. And the computed values are presented in Table 2 and it is clear that α was 9.37 µg/g min while β was 0.28 g/µg; confirming faster sorption than desorption. The degree of the regressing coefficient was 0.939; approaching unity. These data confirmed the applicability of Elovich's kinetic model.

Table 2: Kinetic parameters of triclosan.

Kinetic models and parameters	**Numerical values**
First-second-order	
k_1 (1/min) The experimental Qe (µg/g) The theoretical Qe (µg/g) R^2	0.073 90.2 124.11 0.995
Pseudo-second-order	
k_2 (g/µg min) The experimental Qe (µg/g) The theoretical Qe (µg/g) h (µg/g min) R^2	3.26×10^{-6} 90.2 909.09 2.70 0.994
Elovich	
α (µg/g min) β (g/µg) R^2	9.37 0.028 0.939

3.6 Thermodynamics study

Triclosan sorption thermodynamics of the adsorption phenomenon was ascertained by the thermodynamics equations, which are given in the supplementary information. The thermodynamics was estimated in terms of entropy, enthalpy and free energy. The degrees of entropy and enthalpy were 0.47, and -0.11 and -5.43×10^{-2}, respectively. The degrees of free energy

at 20, 25 and 30 °C were -53.18, -74.17 and -76.14, respectively. The negative values of enthalpy, free energy and entropy are an indication of impulsive sorption and exothermic process.

3.7 Adsorption mechanism

In scientific discoveries, the mechanism of any phenomenon is very important and it is also true with this manuscript. The mechanism of triclosan sorption on *N*-methyl butyl imidazolium bromide copper oxide nanocomposite was studied by exploiting the liquid film diffusion kinetic model and the intra-particle diffusion kinetic models (Figure 7a and b). The equations of the liquid film diffusion kinetic model and the intra-particle diffusion kinetic models are given in supplementary information (Table S2) and these equations were used to model the experimental data. The liquid film diffusion kinetic model parameters were determined and expressed by the rate constant (1/min), intercept and regression constant. The magnitude of the rate constant was exploited by the slope of the plot drawn between t vs ln(1-F) This value is presented in Table 3, which confirmed 0.073 1/min. The magnitude of regressing constant was 0.946 with 0.32 as the intercept value. This information shows that the graph is approaching its origin. Contrarily, the intra-particle diffusion kinetic model parameters were determined and expressed by the rate constant (k_{ipd1}), intercept and regression constant. The magnitude of this constant was exploited by the slope of the plot drawn between Qt *vs* $t^{0.5}$ (Figure 8a and b). The values are presented in Table 3, which confirmed 23.37 k_{ipd1}. The magnitude of regressing constant was 0.976 with -43.72 as the intercept value. This information shows that the graph is not going through the origin. By comparing both models it was found that the graph of the liquid film diffusion kinetic model is passing closer to the origin in comparison to the intra-particle diffusion kinetic model. Moreover, the value of the regression constant was greater in the former model in comparison to the latter. These findings are clear proof of the applicability of the liquid film diffusion kinetic model in the present sorption process.

Table 3: The values of the uptake mechanism parameters of triclosan.

The kinetic models and parameters	Numerical values
The intraparticle diffusion kinetic model	
k_{id} (µg/g $min^{0.5}$) Intercept R^2	23.37 -43.72 0.976
Liquid film diffusion kinetic model	
k_{fd} (1/min) Intercept R^2	0.073 0.32 0.946

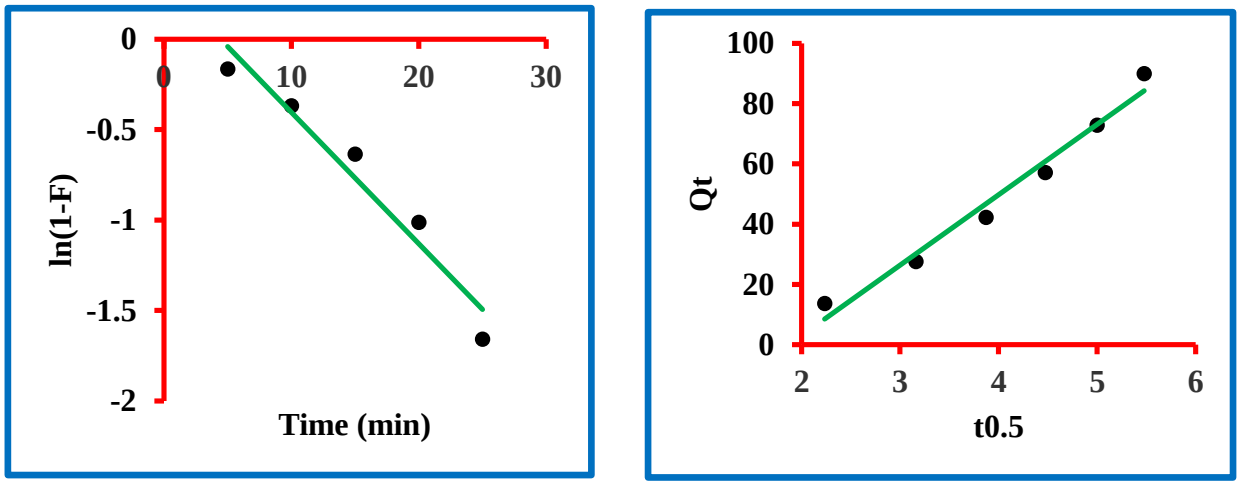

(a) **(b)**

Figure 8. Mechanism of the sorption, (a): liquid film diffusion and (b): intra particular diffusion models.

3.8 Supramolecular mechanism of uptake

Besides using the sorption mechanism model, it is also interesting if the sorption mechanism is developed and this is possible by a simulation study and triclosan and N-methyl butyl imidazolium bromide ionic liquid chemistry. The procedure for simulation between triclosan and N-methyl butyl imidazolium bromide is given in Supplementary information. The outcomes of the binding were calculated in terms of bonding and residues involved. The model developed after simulation between triclosan and N-methyl butyl imidazolium bromide and by chemical

methods is shown in Figure 9. This Figure indicates bonding between the hydroxyl group of triclosan and imidazole ring of N-methyl butyl imidazolium bromide. The maximum adsorption was observed at pH 8.0 and it can be explained at the supramolecular level by considering the model presented in Figure 9. The pKa value of N-methyl butyl imidazolium bromide is 7.0-7.4 and it means that N-methyl butyl imidazolium bromide ionizes at pH 7.0-7.4; leading to the formation of cation of N-methyl butyl imidazolium bromide. On the other hand, the pKa value of 7.9-8.1 and means that triclosan ionizes at 7.9-8.1 pHs; leading to the formation of the anion of triclosan. Finally, the cation and anion interacted by electrovalent bonding and formed a complex structure as shown in Figure 9. Also, it is important to mention that the pKa value of triclosan is controlling sorption because the pKa value of triclosan is higher than the pKa value of N-methyl butyl imidazolium bromide. The residues involved in the formation of the complex structure are the phenoxide group of triclosan and imidazolium ring of N-methyl butyl imidazolium bromide. These interpretations are in good arrangement for supporting the adsorption behavior of the triclosan. Finally, the uptake mechanism at the supramolecular scale is developed and established.

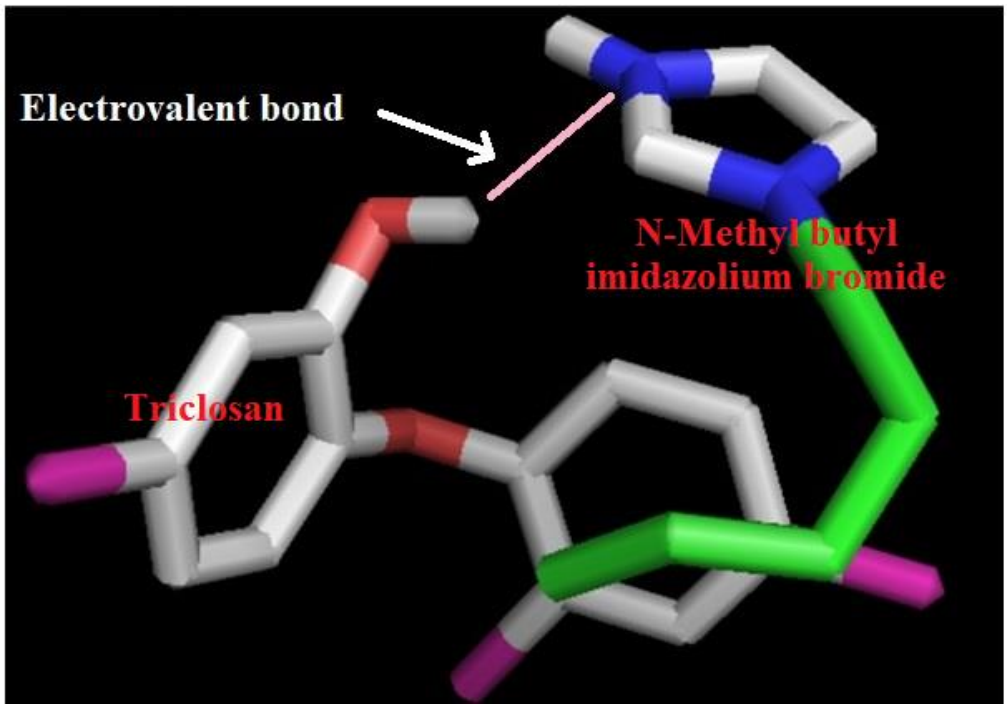

Figure 9: Interacting model of triclosan with N-methyl butyl imidazolium bromide.

4. Conclusions

Copper oxide nanoparticles were synthesized by green methods and the nanocomposite was prepared by using N-methyl butyl imidazolium bromide ionic liquid. The nanocomposite was characterized by using proper spectroscopic methods. The nanocomposite was used to remove triclosan in water and the percentage removal was 90.2% at pH 8.0; which is an asset for using this method in natural water conditions. Besides, 30 minutes is the fast time to apply the method under natural situations. The conditions developed this method were time 30 minutes, concentration 100 µg/L, pH 8.0, dose 1.0 g/L, and 25 °C temperature. The results were verified by Langmuir isotherm. Besides, Temkin and Temkin and D-Rs models were followed well by the data. The sorption mechanism was through the liquid film diffusion kinetic model. The enthalpy and free energy values were negative while the entropy of the value was positive, which confirmed the natural sorption phenomenon at all the working temperatures. Besides, these results also confirmed the exothermic elimination of triclosan. The supramolecular simulation study has confirmed electrostatic interaction between triclosan and N-methyl butyl imidazolium bromide ionic liquid. This method is green in nature and economical in behavior giving 90% elimination of triclosan. Finally, this method is considered worthwhile for the elimination of triclosan in water.

5. Conflict of Interest

The authors of this manuscript do not have any interest in conflict.

References:

1. Olaniyan LWB, Mkwetshana N , Okoh A I (2016) Triclosan in water, implications for human and environmental health, Springerplus 5: 1639.

2. Sarkar SD, Nag SK, Kumari K, Saha K, Bandyopadhyay S, Aftabuddin M, Das BK, (2020) Occurrence and safety evaluation of antimicrobial compounds triclosan and triclocarban in water and fishes of the multitrophic Niche of river Torsa India. Arch Environ Contam & Toxicol 79: 488-499.

3. Vimalkumar K, Arun E, Kumar S K, Poopal R K, Nikhil N P, Subramanian A, Babu-Rajendran R (2018) Occurrence of triclocarban and benzotriazole ultraviolet stabilizers in water, sediment, and fish from Indian rivers. Sci Total Environ 625: 1351–1360.

4. MacIsaac J K, Gerona R R, Blanc P D, Apatira L, Friesen M W, Cop-polino M, Janssen S (2014) Health care worker exposures to the antibacterial agent triclosan. J Occup Environ Med 56: 834-839.

5. Schweizer H P (2001) Triclosan: a widely used biocide and its link to antibiotics. FEMS Microbiol Lett 202: 1–7.

6. Kolpin D W, Furlong E T, Meyer M T, Thurman E M, Zaugg S D, Barber L B, Buxton H T (2000) Pharmaceuticals, hormones, and other organic wastewater contaminants in U S streams, 1999–2000: A national reconnaissance. Environ Sci Technol 36: 1202-1211.

7. Reiss R, Mackay N, Habig C, Griffin J (2002) An ecological risk assessment for triclosan in lotic systems following discharge from wastewater treatment plants in the United States. Environ Toxicol Chem 21: 2483-2492.

8 Loraine G A, Pettigrove M E (2006) Seasonal variations in concentrations of pharmaceuticals and personal care products in drinking water and reclaimed wastewater in southern California. Environ Sci Technol 40: 687-695

9. Li X, Ying G G, Su H C, Yang X B, Wang L (2010) Simultaneous determination and assessment of 4-nonylphenol, bisphenol A and triclosan in tap water, bottled water and baby bottles. Environ Int 36: 557-562.

10. Helbing C C, Aggelen van G , Veldhoen N (2011) Triclosan affects thyroid hormone dependent metamorphosis in anurans. Toxicol Sci 119: 417-418.

11. Park H G, Yeo M K (2012) The toxicity of triclosan, bisphenol a, bisphenol a diglycidyl ether to the regeneration of cnidarian, *Hydra magnipapillata*. Mol Cell Toxicol 8: 209-216.

12. Crofton K M, Paul K B, DeVito M J, Joan M, Hedge J M (2007) Short-term in vivo exposure to the water contaminant triclosan: evidence for disruption of thyroxine. Environ Toxicol Pharmacol 24: 194-197.

13. Huang H, Du G, Zhang W, Hu J, Wu D I, Song L, Xia Y, Wang X (2014) The in vitro estrogenic activities of triclosan and triclocarban. J Appl Toxicol 34: 1060-7.

14. Stoker T E, Gibson E K, Zorrilla L M (2010) Triclosan exposure modulates estrogen-dependent responses in the female Wistar rat. Toxicol Sci 117: 45-53.

15. Ishibashi H, Matsumura N, Hirano M, Matsuoka M, Shiratsuchi H, Ishibashi Y, Takao Y, Arizono K (2004) Effects of triclosan on the early life stages and reproduction of medaka Oryzias latipes and induction of hepatic vitellogenin. Aquat Toxicol 67: 167-179.

16. Fang J L, Vanlandingham M, da Costa G G, Beland F A (2014) Absorption and metabolism of triclosan after application to the skin of B6C3F1 mice, Environ. Toxicol 31: 609-23.

17. Queckenberg C, Meins J, Wachall B, Doroshyenko O, Tomalik-Scharte D, Bastian B, Abdel-Tawab M, Fuhr U (2010) Absorption, pharmacokinetics, and safety of triclosan after dermal administration. Antimic Agent Chemother 54: 570-572.

18. Ali I, Alharbi O M L, ALOthman Z A, Badjah A Y (2018) Kinetics, thermodynamics and modeling of amido black dye photo-degradation in water using Co/TiO_2 nanoparticles. Photochem & Photobiol 94: 935-941.

19. Ali I, Alharbi O M L, ALOthman Z A, Alwarthan A, Al-Mohaimeed A M (2019) Preparation of a carboxymethylcellulose-iron composite for the uptake of atorvastatin in water. Int J Biol Macromol 132: 244-253.

20. Ali I, Burakov A E, Melezhik A V, Babkin A V, Burakova I V, Neskomornaya E A, Galunin E V, Tkachev A G, Kuznetsov D V (2019) Kinetics, thermodynamics and mechanism of copper and zinc metal ions removal in water on newly synthesized polyhydroquinone/graphene nanocomposite material. ChemSelect 4: 12708-12718.

21. Burakova I V, Burakov A E, Tkachev A G, Troshkina I D, Veselova O A, Babkin A V, Aung WM, Ali I (2018) Kinetics of the adsorption of scandium and cerium ions in sulfuric acid solutions on a nanomodified activated carbon. J Mol Liq 253: 277-283.

22. Ali I, Zakharchenko E A, Myasoedova G V, Molochnikova N P, Rodionova A A, Baulin V E, Burakov A E, Burakova I V, Babkin A V, Neskoromnaya E A, Melezhik A V, Tkachev A G, Habila M A, El-Marghany A, Sheikh M, Ghfar A (2021) Preparation and characterization of oxidized graphene for actinides and rare earth elements removal in nitric acid solutions from nuclear wastes. J Mol Liq 335: 116260.

23. Brose D A, Kumar K, Liao A, Hundal L S, Tian G, Cox A, Zhang H, Podczerwinski E W (2019) A reduction in triclosan and triclocarban in water resource recovery facilities' influent, effluent, and biosolids following the U S Food and Drug Administration's 2013 proposed rulemaking on antibacterial products. Water Environ Res 91: 715-721.

24. Wu C, Spongberg A L, Witter J D (2009) Adsorption and Degradation of Triclosan and Triclocarban in Soils and Biosolids-Amended Soils. J Agric Food Chem 57: 4900–4905.

25. Tonga Y , Mayera B K, McNamara P J (2016) Triclosan adsorption using wastewater biosolids-deried biochar. Environ Sci: Water Res Technol 2: 761-768.

26. Khori N K E M, Hadibarata T, Elshikh M S, Al-Ghamdi A A, Yusop SZ (2018) Triclosan removal by adsorption using activated carbon derived from waste biomass: Isotherms and kinetic studies. J Chin Chem Soc 65: 951-959.

27. Fard M A, Barkdoll B (2018) Using recyclable magnetic carbon nanotube to remove micropollutants from aqueous solutions. J Mol Liq 249: 193-202.

28. Li Y, Zhang H, Chen Y, Huang L, Lin Z, Cai Z (2019) Core-shell structured magnetic covalent organic framework nanocomposites for triclosan and triclocarban adsorption. ACS Appl Mater Interfac 11: 22492-22500.

29. Triwiswaraa M, Leeb C G, Moonc J K, Park S J (2020) Adsorption of triclosan from aqueous solution onto char derived from palm kernel shell. Desal & Water Treat 177: 71-79.

30. Jiang N, Shang R, Heijman S G J, Rietveld L C (2020) Adsorption of triclosan, trichlorophenol and phenol by high-silica zeolites: Adsorption efficiencies and mechanisms. Sepn & Purifn Technol 235: 116152.

31. Zheng L, Liu X (2007) Solution phase synthesis of CuO hierarchical nanosheets at near neutral PH and near room temperature. Mater Lett 61: 2222-2226.

32. Wu W, Li W, Han B, Zhang Z, Jiang T, Liu Z (2005) A green and effective method to synthesize ionic liquids: supercritical CO2 route. Green Chem 7: 701-704.